Dept. of Math. Univ. of Oslo
Pure Mathematics No. 35
ISSN 0806–2439 November 2005

Perpetual integral functionals of diffusions and their numerical computations

Paavo Salminen
Åbo Akademi,
Mathematical Department,
Vänriksgatan 3 B,
FIN-20500 Åbo, Finland,
email: phsalmin@abo.fi

Olli Wallin
University of Oslo,
Centre for Mathematics and Applications,
P.O. Box 1053 Blindern,
NO-0316 Oslo, Norway
email: olli.wallin@cma.uio.no

Abstract

In this paper we study perpetual integral functionals of diffusions. Our interest is focused on cases where such functionals can be expressed as first hitting times for some other diffusions. In particular, we generalize the result in [24] in which one-sided functionals of Brownian motion with drift are connected with first hitting times of reflecting diffusions.

Interpretating perpetual integral functionals as hitting times allows us to compute numerically their distributions by applying numerical algorithms for hitting times. Hereby, we discuss two approaches:

- numerical inversion of the Laplace transform of the first hitting time,
- numerical solution of the PDE associated with the distribution function of the first hitting time.

For numerical inversion of Laplace tranforms we have implemented the Euler algorithm developed by Abate and Whitt. However, perpetuities lead often to diffusions for which the explicit forms of the Laplace transforms of first hitting times are not available. In such cases, and also otherwise, algorithms for numerical solutions of PDE's can be evoked. In particular, we analyze the Kolmogorov PDE of some diffusions appearing in our work via the Crank-Nicolson scheme.

Keywords: Bessel process, geometric Brownian motion, random time change, local time.

AMS Classification: 60J65, 60J60, 62E25.

1 Introduction

Let $\{Y_t : t \geq 0\}$ be a regular linear diffusion taking values on an interval I. The left and right endpoints of the interval are denoted by l and r, respectively. For a locally integrable function $f : I \mapsto \mathbf{R}_+$ define the perpetual integral functional associated with f and Y via

$$\int_0^\infty f(Y_t)\, dt. \tag{1.1}$$

An important example of perpetual integral functionals is

$$\int_0^\infty \exp\left(-2a\, B_t^{(\mu)}\right)\, dt, \quad a > 0,$$

where $B^{(\mu)}$ is a BM with positive drift μ, studied by Dufresne in [10] in connection with risk theory and pension funding. In particular, from [10], this functional is distributed as $1/(2\, a^2\, Z_\nu)$ where Z_ν is a gamma-distributed random variable with the density function

$$f_{Z_\nu}(z) = \frac{1}{\Gamma(\nu)}\, z^{\nu-1} \mathrm{e}^{-z}, \quad \nu := \mu/a.$$

In Yor [31] (see [32] for an English translation) it is shown

$$\int_0^\infty \exp(-2aB_s^{(\mu)})\, ds \quad \stackrel{(\mathrm{d})}{=} \quad H_0(R^{(\delta)}), \tag{1.2}$$

where $R^{(\delta)}$ is a Bessel process of dimension $\delta = 2(1 - (\mu/a))$ started at $1/a$,

$$H_0(R^{(\delta)}) := \inf\{t : \ R_t^{(\delta)} = 0\},$$

and $\stackrel{(\mathrm{d})}{=}$ reads "is identical in law with" (in fact, $R^{(\delta)}$ can be constructed in the same probability space as $B^{(\mu)}$ and then (1.2) holds a.s.). In [24] the methodology used in [31] is developed for more general perpetual functionals for BM with positive drift and, in particular, results for one sided functionals are presented. An example of these is

$$\int_0^\infty \exp(-2aB_s^{(\mu)})\, \mathbf{1}_{\{B_s^{(\mu)} > 0\}} ds \quad \stackrel{(\mathrm{d})}{=} \quad H_{1/a}(R^{(2\mu/a)}),$$

where the Bessel diffusion $R^{(2\mu/a)}$ is started at 0 and, in the case $0 < \mu < a$, reflected at 0. For further results and references for Dufresne's functionals, see [26], [20], [23], [24] and [9].

In this paper, Section 2, we recall (from [4]) the connection between perpetual integral functionals and first hitting times. After this, the result in [24], Proposition 2.3, concerning one-sided perpetual functionals of $B^{(\mu)}$ is generalized for Y (defined via a SDE) and functionals of the type in (1.1). In Section 3, to make the paper more self contained and also as an introduction to Section 4, some basic facts about the distributions of the first

hitting times are presented. Section 4 contains brief descriptions of the Euler algorithm for numerical inversion of Laplace transforms and the Crank-Nicolson scheme for solving PDE's, which we implemented in Matlab. The paper is concluded with Section 5 where the distributions of some perpetual functionals are computed numerically. In particular, we compare the one-sided functionals

$$\int_0^\infty \exp(-2B_s^{(\mu,\sigma)}))\,\mathbf{1}_{\{B_s^{(\mu,\sigma)}>0\}}\,ds \quad \text{and} \quad \int_0^\infty (1+\exp(B_s^{(\mu,\sigma)}))^{-2}\,\mathbf{1}_{\{B_s^{(\mu,\sigma)}>0\}}\,ds,$$

where $B_t^{(\mu,\sigma)} := \sigma\, B_t + \mu\, t$ with B the standard Brownian motion. It is also seen that some of the diffusions studied have bad singularities making the PDE's numerically troublesome to solve. In some cases this problem can, at least partly, be solved by transforming the diffusion to a new one with better behaviour. It seems to us that for a general numerical approach for calculating distributions of perpetualities, more sophisticated PDE or other methods such as Monte Carlo simulation are needed for the cases where the Laplace transform is not available for numerical inversion.

2 Perpetual integral functionals as first hitting times

Consider a diffusion Y on an open interval $I = (l, r)$ determined by the SDE

$$dY_t = \sigma(Y_t)\,dB_t + b(Y_t)\,dt, \tag{2.1}$$

where B is a standard Brownian motion defined in a complete probability space $(\Omega, \mathcal{F}, \{\mathcal{F}_t\}, \mathbf{P})$. It is assumed that σ and b are continuous and $\sigma(x) > 0$ for all $x \in I$. The diffusion Y is considered up to its explosion (or life) time

$$\zeta := \inf\{t \ : \ Y_t \notin I\}.$$

Let f be a positive and continuous function defined on I, and consider for $t \geq 0$ the integral functional

$$A_t := \int_0^t f(Y_s)\,ds.$$

We remark that $\{A_t \ : \ t \geq 0\}$ is an additive functional of Y in the usual sense (see e.g. [2] p. 148). Taking $t = \zeta$ gives us the perpetual integral functional

$$A_\zeta := \int_0^\zeta f(Y_s)\,ds.$$

Assuming that $A_\zeta < \infty$ a.s. we are interested in the distribution of A_ζ.

A sufficient condition for finiteness is clearly that the mean of A_ζ is finite:

$$\begin{aligned}\mathbf{E}_x\,(A_\zeta) &= \int_0^\infty \mathbf{E}_x\,(f(Y_s))\;ds \\ &= \int_l^r G_0(x,y)\,f(y)\,m(dy) < \infty,\end{aligned}$$

where G_0 denotes the Green kernel of Y and m is the speed measure (for these see, e.g., [3]). A neccessary and sufficient condition in the case of a Brownian motion with drift $\mu > 0$ is that the function f is integrable at $+\infty$ (see Engelbert and Senf [11] and Salminen and Yor [25]). We refer also to a recent paper [22] for such a condition valid for continuous f and a fairly general diffusion Y.

Next proposition connects the perpetual integral functionals to the first hitting times. The result is extracted from Propositions 2.1 and 2.3 in [4] where the proof can be found. We remark also that the result generalizes Proposition 2.1 in [24].

Proposition 2.1. *Let Y, A, and f be as above and assume that there exists a two times continuously differentiable function g such that*

$$f(x) = \big(g'(x)\sigma(x)\big)^2, \quad x \in I. \tag{2.2}$$

Let $\{a_t : 0 \le t < A_\zeta\}$ denote the inverse of A, that is,

$$a_t := \min\big\{s : A_s > t\big\}, \qquad t \in [0, A_\zeta).$$

1. *Then the process Z given by*

$$Z_t := g\left(Y_{a_t}\right), \qquad t \in [0, A_\zeta), \tag{2.3}$$

is a diffusion satisfying the SDE

$$dZ_t = d\widetilde{B}_t + G(g^{-1}(Z_t))\, dt, \qquad t \in [0, A_\zeta).$$

where $\widetilde{B}_t$ is a Brownian motion and

$$G(x) = \frac{1}{f(x)}\left(\frac{1}{2}\,\sigma(x)^2\, g''(x) + b(x)\, g'(x)\right). \tag{2.4}$$

2. *Let $x \in I$ and $y \in I$ be such that $\mathbf{P}_x$-a.s.*

$$H_y(Y) := \inf\{t : Y_t = y\} < \infty.$$

Then

$$A_{H_y(Y)} = \inf\{t : Z_t = g(y)\} =: H_{g(y)}(Z) \quad a.s.$$

with $Y_0 = x$ and $Z_0 = g(x)$.

3. *Suppose $g(r) := \lim_{z\to r} g(z)$ exists. Suppose also that the following statements hold a.s.*

$$(i) \quad \lim_{t\to\zeta} Y_t = r, \quad (ii) \quad A_\zeta := \lim_{t\to\zeta} A_t < \infty.$$

Then

$$A_\zeta = H_{g(r)}(Z) \quad a.s.$$

In [24] Proposition 2.3 one sided functionals for Brownian motion with positive drift are studied. This result is generalized here, under some assumptions, to the present case. Suppose $0 \in (l, r)$ and recall that $f(x) > 0$ for all $x \in (l, r)$. Consider the functional

$$A^0_\zeta := \int_0^\zeta f(Y_s)\, \mathbf{1}_{\{Y_s>0\}}\, ds.$$

Let

$$C_t := \int_0^t \mathbf{1}_{\{Y_s>0\}}\, ds, \quad t \le \zeta,$$

and $\{c_t \,:\, 0 \le t < B_\zeta\}$ denote the inverse of C. We assume also that

$$\lim_{t\to\zeta} Y_t = r \quad \text{a.s.} \tag{2.5}$$

It is well known (see [15]) that the process

$$Y^+ := \{Y_{c_t} \,:\, 0 \le t < C_\zeta\}$$

is identical in law with Y living on $[0, r)$ and having 0 as a reflecting boundary point. Applying the random time change means that on every sample path the excursions below 0 are omitted after which the gaps created are closed by joining the excursions together. Therefore,

$$A^0_\zeta = \int_0^{\zeta^+} f(Y^+_s)\, ds =: A^+_\zeta$$

where ζ^+ is the life time of Y^+.

Next introduce the local time of Y^+ at 0 via

$$L_t(Y^+) := \sigma^2(0) \lim_{\varepsilon\downarrow 0} (2\varepsilon)^{-1} \mathrm{Leb}\{0 \le s \le t \,:\, Y^+_s < \varepsilon\}.$$

Under some additional smoothness assumptions on σ and b (see McKean [19]) the pair $(Y^+, L(Y^+))$ with $Y^+_0 = x > 0$ can be viewed as the unique solution of the reflected SDE

$$dX_t = \sigma(X_t)\, dB_t + b(X_t)\, dt + dL_t(X), \quad X_0 = x,$$

such that

(a) $\lim_{t\to\zeta(X)} X(t) = r$,

(b) $0 \le X(t) < r$ for all $t < \zeta(X)$,

(c) $t \mapsto L_t(X)$ is continuous, increasing with $L_0(X) = 0$, and

$$\int_0^t \mathbf{1}_{\{0\}}(X_s)\, dL_s(X) = L_t(X).$$

We now give the promised generalization.

Proposition 2.2. *Let Y^+ be as given above and define for $t < \zeta^+$*

$$A_t^+ := \int_0^t f(Y_s^+)\, ds.$$

The inverse of A^+ is denoted by $\{a_t^+ \,:\, 0 \le t < A_\zeta\}$. Recall the definition of the function g in (2.2) and define the process Z^+ via

$$Z_t^+ := g\left(Y_{a_t^+}^+\right), \qquad t \in [0, A_\zeta^+). \tag{2.6}$$

Then

$$A_\zeta^+ = \inf\{t \,:\, Z_t^+ = g(r)\} \quad \text{a.s.} \tag{2.7}$$

with $Z_0 = g(x)$. Moreover, Z^+ satisfies the reflected SDE

$$dZ_t^+ = d\widetilde{B}_t + G(g^{-1}(Z_t^+))\, dt + dL_t(Z^+), \qquad t \in [0, A_\zeta^+). \tag{2.8}$$

where $\widetilde{B}_t$ is a Brownian motion,

$$L_t(Z^+) = \lim_{\varepsilon \downarrow 0} (2\varepsilon)^{-1} \mathrm{Leb}\{0 \le s \le t \,:\, g(0) \le Z_s^+ < g(0) + \varepsilon\}, \tag{2.9}$$

and G is as in (2.4). The local time $L(Z^+)$ is related to the local time $L(Y^+)$ by

$$L_t(Z^+) = g'(0) L_{a_t^+}(Y^+). \tag{2.10}$$

Proof. To fix ideas, assume that g is monotonically increasing. By Ito's formula for $u < \zeta$

$$\begin{aligned} g(Y_u^+) - g(Y_0^+) = \int_0^u g'(Y_s^+) \left(\sigma(Y_s^+)\, dB_s + b(Y_s^+)\, ds + dL_s(Y^+)\right) \\ + \frac{1}{2} \int_0^u g''(Y_s^+) \sigma^2(Y_s^+)\, ds. \end{aligned}$$

Replacing u by a_t^+ yields

$$\begin{aligned} Z_t^+ - Z_0^+ = \int_0^{a_t^+} g'(Y_s^+) \sigma(Y_s^+)\, dB_s + g'(0)\, L_{a_t^+}(Y^+) \\ + \int_0^{a_t^+} \left(g'(Y_s^+)\sigma(Y_s^+)\right)^2 G(Y_s^+)\, ds. \end{aligned}$$

Since a_t^+ is the inverse of A_t^+ and $(A_s^+)' = \left(g'(Y_s^+)\sigma(Y_s^+)\right)^2$ we have

$$(a_t^+)' = \frac{1}{(A_{a_t^+}^+)'} = \left(g'(Y_{a_t^+}^+)\sigma(Y_{a_t^+}^+)\right)^{-2}. \tag{2.11}$$

From Lévy's theorem it follows that

$$\widetilde{B}_t := \int_0^{a_t^+} g'(Y_s^+)\sigma(Y_s^+)\,dB_s, \qquad t \in [0, A_\zeta^+),$$

is a (stopped) Brownian motion. Consequently, for $t < A_\zeta^+$

$$\begin{aligned} Z_t^+ - Z_0^+ &= \widetilde{B}_t + g'(0)\,L_{a_t^+}(Y^+) + \int_0^t \big(g'(Y^+_{a_s^+})\sigma(Y^+_{a_s^+})\big)^2 G(Y^+_{a_s^+})\,da_s^+ \\ &= \widetilde{B}_t + \int_0^t G(g^{-1}(Z_s^+))\,ds + g'(0)\,L_{a_t^+}(Y^+). \end{aligned}$$

Clearly, viewing $t \mapsto g'(0)\,L_{a_t^+}(Y^+)$ as a functional of Z^+ then this functional increases only on the set $\{t.:\ Z_t^+ = g(0)\}$. Moreover, since $Y_t^+ \geq 0$ for $t \geq 0$ we have $Z_t^+ \geq g(0)$ for $t \geq 0$ by monotonicity of g. Hence, $(Z^+, L(Z^+))$ can be seen as the unique solution of the reflected SDE (2.8) with $L(Z^+)$ as in (2.9) satisfying (2.10), as claimed. Finally, again by the monotonicity of g, the identity (2.7) follows from the definition (2.6) of Z^+ and the assumption (2.5). □

Remark 2.3. *Notice that the above approach yields a stronger result than in [24], i.e., the identity (2.7) holds a.s.*

3 Reminder on first hitting times

3.1 Distribution functions and PDEs

Let Y be a linear diffusion determined via the SDE (2.1). It is here assumed that Y hits r a.s. and is killed when this happens. Therefore, the boundary point r is either exit-not-entrance or regular with killing, and l is either natural or entrance-not-exit or regular with reflection. Letting $H_r(Y)$ denote the hitting time of r we have

$$\mathbf{P}_x(H_r(Y) > t) = \int_l^r p(t;x,y)\,m(dy), \tag{3.1}$$

where p denotes the symmetric transition density of Y with respect to its speed measure m. It is well known (see [15] p. 149 and [18]) that $(t,x) \mapsto p(t;x,y)$ satisfies for all $y \in (l,r)$ the PDE

$$\begin{aligned} \frac{\partial}{\partial t}p(t;x,y) &= \frac{1}{2}\sigma^2(x)\,\frac{\partial^2}{\partial x^2}p(t;x,y) + b(x)\,\frac{\partial}{\partial x}p(t;x,y) \\ &=: (\mathcal{G}\,p)(t;x,y) \end{aligned}$$

and the condition $\lim_{x\to r} p(t;x,y) = 0$. Moreover, in the case l is regular with reflection or entrance-not-exit we impose at l the condition

$$\lim_{x\to l}\frac{\partial}{\partial x}p(t;x,y) = 0,$$

and in the case l is natural the condition

$$\lim_{x\to l} p(t;x,y) = \lim_{x\to l} \frac{\partial}{\partial x} p(t;x,y) = 0.$$

See [15] or [3] for the boundary classification of linear diffusions.

Letting $\{T_t\}$ denote the semigroup associated with Y we may write from (3.1)

$$\mathbf{P}_x(H_r(Y) > t) = T_t 1(x).$$

Recall from [18] (where the case with natural scale is treated) that $(t,x) \mapsto T_t g(x)$ with g bounded and continuous satisfies

$$\frac{\partial}{\partial t}(T_t g)(x) = (\mathcal{G}\, T_t) g(x).$$

Consequently, the distribution function

$$(t,x) \mapsto u(t,x) := \mathbf{P}_x(H_z(Y) < t)$$

is the unique solution of the PDE problem

$$\frac{\partial}{\partial t} u(t,x) = (\mathcal{G}\, u)(t,x) \tag{3.2}$$

with the initial condition $\lim_{t\to 0} u(t,x) = 0 \quad$ for all $x \in (l,r)$ and the boundary condition $\lim_{x\to r} u(t,x) = 1 \quad$ for all $t > 0$. Further, if l is regular with reflection or entrance-not-exit

$$\lim_{x\to l} \frac{\partial}{\partial x} u(t,x) = 0,$$

and in the case l is natural

$$\lim_{x\to l} u(t,x) = \lim_{x\to l} \frac{\partial}{\partial x} u(t,x) = 0.$$

Remark 3.1. *Using the fact (see [18]) that*

$$(t,x,y) \mapsto \frac{\partial}{\partial t} p(t;x,y)$$

is continuous and satisfies the same boundary conditions as the density $p(t;x,y)$ it is easy (at least when $m(l,r) < \infty$) to deduce that

$$\frac{\partial}{\partial t} \mathbf{P}_x(H_z(Y) < t) = -\lim_{y\to z} \frac{1}{S'(y)} \frac{\partial}{\partial y} p(t;x,y),$$

where

$$S'(y) = \exp\left(-\int^y 2\,\sigma^{-2}(v)\, b(v)\, dv \right)$$

is the derivative of the scale function S (cf. [15] p. 154).

3.2 Laplace transforms and ODEs

For the approach with the Laplace transform of $H_r(Y)$ consider the second order ODE

$$\mathcal{G}u(x) = \lambda u(x), \tag{3.3}$$

where $\lambda \geq 0$. It is known (see [12] p. 488, and [15] p. 128) that the equation (3.3) has a positive increasing solution ψ_λ and a positive decreasing solution φ_λ. In case l is natural or entrance and r is exit these solutions are unique up to multiplicative constants. When l is regular with reflection the condition $\psi'_\lambda(l) = 0$ must be posed, and when r is regular with killing the condition is $\varphi_\lambda(r-) = 0$. The Green kernel G_λ of Y can be expressed via these solutions as

$$\begin{aligned} G_\lambda(x,y) &:= \int_0^\infty \mathrm{e}^{-\lambda t}\, p(t;x,y)\, dt \\ &= \begin{cases} \frac{1}{w_\lambda}\, \psi_\lambda(x)\, \varphi_\lambda(y), & x \leq y, \\ \frac{1}{w_\lambda}\, \psi_\lambda(y)\, \varphi_\lambda(x), & y \leq x, \end{cases} \end{aligned}$$

where w_λ is the Wronskian (see e.g. [3]). Using the Green kernel the Laplace transform for the first hitting time $H_y(Y)$ is given by

$$\mathbf{E}_x\left(\mathrm{e}^{-\lambda H_y(Y)}\right) = \frac{G_\lambda(x,y)}{G_\lambda(y,y)}$$

and, in particular,

$$\mathbf{E}_x\left(\mathrm{e}^{-\lambda H_r(Y)}\right) = \frac{\psi_\lambda(x)}{\psi_\lambda(r)}. \tag{3.4}$$

4 Numerical methods

4.1 Numerical inversion of Laplace transforms

There are several efficient methods for numerical inversion of the Laplace transforms of probability density functions or probability distribution functions. We have implemented a method developed by Abate and Whitt in [1]. This so called the Euler-algorithm has proved to be very effective in many applications see e.g. [13], [6], [7] and [8]. The main features of this method are presented below. For more details and also for further references, see [1].

Consider a non-negative random variable with density f and its Laplace transform

$$\hat{f}(\lambda) := \int_0^\infty \mathrm{e}^{-\lambda t}\, f(t)\, dt.$$

The well known inversion integral formula (called the Bromwich or also the Fourier-Mellin integral) states that

$$f(t) = \frac{1}{2\pi\,\mathrm{i}} \int_{a-\mathrm{i}\,\infty}^{a+\mathrm{i}\,\infty} \mathrm{e}^{\lambda t}\, \hat{f}(\lambda)\, d\lambda, \tag{4.1}$$

where it is assumed that $\hat{f}$ does not have singularities on or to the right of the vertical line $\lambda = a$.

Remark 4.1. *For first hitting times of diffusions considered in Section 3 we have (cf. (3.4))*

$$\hat{f}(\lambda) = \mathbf{E}_x\left(\mathrm{e}^{-\lambda H_r(Y)}\right) = \frac{\psi_\lambda(x)}{\psi_\lambda(r)}.$$

If the left boundary point l is not natural it follows from the classical theory of second order differential operators (see e.g. [16]) that $\psi_\lambda(x)$ is for every $x \in (l, r)$ an entire function of λ and the zeroes of $\lambda \mapsto \psi_\lambda(x)$ are for every $x \in (l, r)$ simple and negative. Consequently, the inversion formula (4.1) holds in this case for any $a > 0$. If l is natural we can approximate the first hitting time $H_r(Y)$ via a sequence of first hitting times $\{H_r(Y^{(n)})\}$ associated with the diffusions $Y^{(n)}$, $n = 1, 2, \ldots$, constructed from Y by reflection at $l + \frac{1}{n}$, respectively. Then $H_r(Y^{(n)}) \to H_r(Y)$ in distribution and by dominated convergence it is seen that (4.1) is valid also in this case.

Since $\mathrm{Re}(\hat{f}(a + \mathrm{i}\,u)) = \mathrm{Re}(\hat{f}(a - \mathrm{i}\,u))$, $\mathrm{Im}(\hat{f}(a + \mathrm{i}\,u)) = -\mathrm{Im}(\hat{f}(a - \mathrm{i}\,u))$, and $f(t) = 0$ for $t < 0$ the inversion integral (4.1) takes the form

$$f(t) = \frac{2\mathrm{e}^{at}}{\pi} \int_0^\infty \mathrm{Re}(\hat{f}(a + \mathrm{i}\,u))\, \cos(ut)\, du. \tag{4.2}$$

Next we approximate $f(t)$ by using the trapezoidal rule for the integral (4.2) (see [1] for some comments on the effectiveness of this procedure). Letting h denote the step size we have for fixed a and t

$$f(t) \approx f_h(t) = \frac{h\mathrm{e}^{at}}{\pi}\,\mathrm{Re}\big(\hat{f}(a)\big) + \frac{2h\mathrm{e}^{at}}{\pi} \sum_{k=1}^{\infty} \mathrm{Re}\big(\hat{f}(a + kh\,\mathrm{i})\big)\cos(kht).$$

Choosing $h = \pi/(2t)$, $a = A/(2t)$ (with A to be made precise later) and truncating the infinite series to the first j terms we are led to define

$$s_j(t) := \frac{\mathrm{e}^{A/2}}{t} \sum_{k=0}^{j} (-1)^k a_k(t), \tag{4.3}$$

where

$$a_0(t) := \hat{f}\,(A/2t)\,/2$$

and

$$a_k(t) := \mathrm{Re}\left(\hat{f}\,((A + 2k\pi\,\mathrm{i})/2t)\right), \quad k = 1, 2, \ldots, j.$$

It is possible to accelerate the convergence of the series in (4.3) by considering it as an alternating series (which is not the case in general) and using the Euler summation with

binomial weights (see [1]). Hence, the proposed final approximation with parameters m, n, and A is

$$f(t) \approx E(m,n,t) := \sum_{k=0}^{m} \binom{m}{k} 2^{-m}\, s_{n+k}(t),$$

In the examples below we use, following [1], $m = 11$ and $n = 15$. The error associated with Euler summation can be estimated by considering the difference

$$E(m, n+1, t) - E(m, n, t).$$

It is advantageous from numerical computational point of view to invert, instead of the density function, the complementary distribution function. Therefore consider

$$\hat{F}^c(\lambda) := \int_0^\infty \mathrm{e}^{-\lambda t}\,(1 - F(t))\,dt,$$

where F is the distribution function associated with f. Firstly, the fact $|1 - F(t)| \leq 1$ can be used to show (see [1]) that

$$|e_d| \leq \frac{\mathrm{e}^{-A}}{1 - \mathrm{e}^{-A}},$$

where e_d stands for the discretization error when approximating the integral in (4.2) for $\hat{F}^c$ via the trapezoidal rule. For instance, $A = 18.4$ gives the upper bound 10^{-8}. Secondly, under some additional smoothness assumption, it can be proved (see [1] Remark 1) that for $\hat{F}^c$ we have $a_k(t) > 0$ when k/t is large enough motivating the use of the Euler summation (since the series in (4.3) is now alternating).

For the first hitting time of r for the diffusion Y the Laplace transform of the complementary distribution function is given by

$$\begin{aligned}\hat{F}^c(\lambda) &= \frac{1}{\lambda}\left(1 - \mathbf{E}_x\left(\mathrm{e}^{-\lambda H_r(Y)}\right)\right) = \frac{1}{\lambda}\left(1 - \frac{\psi_\lambda(x)}{\psi_\lambda(r)}\right) \\ &= \frac{1}{\lambda}\,\frac{\psi_\lambda(r) - \psi_\lambda(x)}{\psi_\lambda(r)}\end{aligned}$$

4.2 Numerical solutions of PDEs

In this section we describe using [28] and [27] two finite difference methods known as the *Crank-Nicolson* (C-N) scheme and the *backward Euler* (BE) method. The C-N scheme is used with satisfactory results in [21] for calculation of transition probability densities of certain diffusions. The BE method can be applied in connection with the C-N scheme for the first time step to damp some numerical oscillations typical to the C-N scheme. Both methods are unconditionally stable: the numerical solutions are well behaved (do not blow up) for any choice of Δt. Because of the singularities appearing in the drift coefficients of our equations, methods that do not have this property (such as the explicit, forward Euler method) are practically unusable since they would require extremely small time steps.

To start with, let us introduce a uniformly spaced grid on the rectangle $[0,T]\times[l,r]$ with $(M+1)\times(N+1)$ nodes, that is, for

$$\Delta t = \frac{T}{M}, \quad \Delta x = \frac{r-l}{N},$$

we let $t_m = m\Delta t$ and $x_n = l + n\Delta x$ where $m = 0,1,...,M$, $n = 0,1,...,N$. For a real valued function f we use the following finite difference approximations, which can be justified with Taylor's expansion:

· the *forward difference* approximation of the derivative of f is

$$\frac{\partial f}{\partial x}(x_i) = \frac{f(x_{i+1}) - f(x_i)}{\Delta x} + \mathcal{O}(\Delta x).$$

· the *centralized difference* approximation of the derivative of f is

$$\frac{\partial f}{\partial x}(x_i) = \frac{f(x_{i+1}) - f(x_{i-1})}{2\Delta x} + \mathcal{O}((\Delta x)^2).$$

· the centralized difference approximation of the second order derivative of f is

$$\frac{\partial^2 f}{\partial x^2}(x_i) = \frac{f(x_{i+1}) - 2f(x_i) + f(x_{i-1})}{(\Delta x)^2} + \mathcal{O}((\Delta x)^2).$$

The C-N scheme approximates the left hand side in equation (3.2) with the forward difference and the right hand side with the average of the centralized differences at two consequtive times. Denoting $u_n^m := u(t_m, x_n)$ and dropping the truncation error terms, the discretized equation then reads

$$\begin{aligned}\frac{u_n^{m+1} - u_n^m}{\Delta t} &= \frac{1}{2}\sigma^2(x_n)\frac{1}{2}\Big(\frac{u_{n+1}^{m+1} - 2u_n^{m+1} + u_{n-1}^{m+1}}{(\Delta x)^2} + \frac{u_{n+1}^m - 2u_n^m + u_{n-1}^m}{(\Delta x)^2}\Big) \\ &+ b(x_n)\frac{1}{2}\Big(\frac{u_{n+1}^{m+1} - u_{n-1}^{m+1}}{2\Delta x} + \frac{u_{n+1}^m - u_{n-1}^m}{2\Delta x}\Big).\end{aligned}$$

Multiply both sides with Δt, and define $r_1 = \frac{\Delta t}{2\Delta x}$, $r_2 = \frac{\Delta t}{2(\Delta x)^2}$. Rearranging the terms so that the values at time t_{m+1} appear on the left hand side and values at time t_m appear on the right hand side, we have

$$A_n u_{n-1}^{m+1} + B_n u_n^{m+1} - C_n u_{n+1}^{m+1} = -A_n u_{n-1}^m + D_n u_n^m + C_n u_{n+1}^m$$

where

$$\begin{aligned}A_n &= \frac{1}{2}\Big(b(x_n)r_1 - \sigma^2(x_n)r_2\Big), &(4.4)\\ B_n &= 1 + \sigma^2(x_n)r_2, &(4.5)\\ C_n &= \frac{1}{2}\Big(b(x_n)r_1 + \sigma^2(x_n)r_2\Big), &(4.6)\\ D_n &= 1 - \sigma^2(x_n)r_2. &(4.7)\end{aligned}$$

Together with the boundary conditions, these form a set of $N+1$ linear equations which we then solve for each $m = 1, 2, ..., M+1$, using the initial condition for $m = 0$. The Neumann boundary condition (which is needed at a reflecting or an entrance boundary point) is implemented with the second order approximation. In other words, from

$$\frac{u_1^m - u_{-1}^m}{2\Delta x} = 0$$

we have $u_{-1}^m = u_1^m$ for the value of u at a "ghost" point beyond the boundary. Plugging this into the discretized equation at $n = 0$ gives

$$(1 + r_2\sigma^2(x_n))u_0^{m+1} - r_2\sigma^2(x_n)u_1^{m+1} = (1 - r_2\sigma^2(x_n))u_0^m + r_2\sigma^2(x_n)u_1^m.$$

Using a second order approximation for the boundary condition seems to be important in order to have good convergence.
For the backward Euler method, one similarly takes the central approximations for the spatial derivatives but now only at the time step $m+1$. This leads to the equation

$$A_n u_{n-1}^{m+1} + B_n u_n^{m+1} - C_n u_{n+1}^{m+1} = u_n^m$$

for $n = 1, ..., N$ and $m = 1, ..., M$, where A_n, B_n, C_n are given in (4.4)-(4.6) but now with $r_1 = \frac{\Delta t}{\Delta x}$, $r_2 = \frac{\Delta t}{(\Delta x)^2}$. The second order implementation of the Neumann boundary condition becomes

$$(1 + r_2\sigma^2(x_n))u_0^{m+1} - r_2\sigma^2(x_n)u_1^{m+1} = u_0^m.$$

Both methods described above are second order accurate in space, but only the C-N scheme is second order accurate in time. However, C-N is known to produce numerical oscillations around discontinuities and sharp gradients if the drift term is large compared to the diffusion coefficient (see for example [5], [14]), while the BE method does not have this problem. In our examples this is seen as oscillations near the killing boundary. Although these oscillations were damped quite rapidly both in space and time, they still produced a small phase shift in the numerical solution of the hitting time distribution $t \mapsto u(x,t)$. For this reason the first step in the C-N scheme is divided into $10 - 100$ substeps, as suggested in [5]. For the substeps we used the BE method. While small oscillations still remained for some of the examples, this procedure provided sufficient damping to give very accurate results in our test cases.

A problem more serious than the oscillations appearing in the C-N scheme is faced when the diffusing particle is pushed away from an exit boundary by a drift term tending to infinity in the vicinity of the boundary. In such cases convergence can be very slow or even nonattainable without huge computer capacity. We discuss this problem in more detail in the examples below.

5 Examples

In this section some perpetuities are examined numerically. If the Laplace transforms of the functionals are available we use the Euler algorithm for computing the density and/or

the distribution functions. Applying in these cases also the numerical methods based on the associated PDE's obtained from the hitting time representations of the functionals and checking that the solutions resulting from the different methods coincide we are able to verify the correctness of the implementations.

Numerical methods for solving PDEs constitute a powerful tool for computing hitting time distributions of diffusions in general. However, there are diffusions as in Example 5.4 for which the methods presented here work unsatisfactorily. At least in some particular cases it is possible to transform the diffusion to a new one for which the methods seem to work better. This is discussed in Example 5.4. Due to these difficulties one may consider the numerical inversion of the Laplace transforms when available as the first choice for the kind of numerical computations studied in the paper.

Below the notation $\{B_t^{(\mu,\sigma)} : t \geq 0\}$ is used for a Brownian motion with (infinitesimal) drift μ and variance σ, i.e., $B_t^{(\mu,\sigma)} = \sigma\, B_t + \mu\, t$ with B a standard Brownian motion. We assume that $\sigma > 0$ and $\mu > 0$. In case $\sigma = 1$ we write $B^{(\mu)}$ for $B^{(\mu,1)}$. For a Bessel process with dimension parameter δ we use the notation of $\{R_t^{(\delta)} : t \geq 0\}$, and refer to [3] for their properties. If nothing else is written it is assumed that $B_0^{(\mu,\sigma)} = 0$ and $R_0^{(\delta)} = 0$.

Example 5.1. Consider the perpetual integral functional

$$I_1 := \int_0^\infty \cosh^{-2}(B_t^{(\mu)})\, dt.$$

The Laplace transform of this functional is computed in [4] and [29] for an arbitrary initial value x; taking therein $x = 0$ gives

$$\mathbf{E}_0\left(\exp\Big(-\rho\, I_1\Big)\right) = K\, {}_2F_1(\alpha, \beta, 1+\mu; 1/2).$$

where

$$\alpha = \frac{1}{2} + \frac{1}{2}\sqrt{1-8\rho}, \quad \beta = \frac{1}{2} - \frac{1}{2}\sqrt{1-8\rho},$$
$$K = \frac{\Gamma(\mu+\alpha)\ \Gamma(\mu+\beta)}{\Gamma(\mu)\ \Gamma(\mu+1)},$$

and ${}_2F_1$ denotes Gauss's hypergeometric function given by

$$\begin{aligned} {}_2F_1(a,b,c;x) &:= \frac{\Gamma(c)}{\Gamma(a)\,\Gamma(b)} \sum_{k=0}^{\infty} \frac{\Gamma(a+k)\,\Gamma(b+k)}{\Gamma(c+k)}\, \frac{x^k}{k!} \\ &= 1 + \sum_{k=1}^{\infty} \frac{a(a+1)\ldots(a+k-1)\, b(b+1)\ldots(b+k-1)}{c(c+1)\ldots(c+k-1)} \frac{x^k}{k!}. \end{aligned}$$

Applying Proposition 2.1 with $g(x) := 2\arctan \mathrm{e}^x$ we obtain

$$I_1 = H_\pi(Z) \qquad a.s.,$$

where Z satisfies

$$dZ_t = dB_t + \left(\frac{1}{2}\operatorname{ctn} Z_t + \frac{\mu}{\sin Z_t}\right) dt, \qquad Z_0 = \pi/2. \tag{5.1}$$

For the drift term in (5.1), it holds

$$G(g^{-1}(x)) = \frac{1}{2}\operatorname{ctn} x + \frac{\mu}{\sin x} = \frac{1}{2}\left(\mu - \frac{1}{2}\right)\tan\frac{x}{2} + \frac{1}{2}\left(\mu + \frac{1}{2}\right)\operatorname{ctn}\frac{x}{2}.$$

Notice that for $0 < \mu < 1/2$ the drift of Z tends to $-\infty$ when Z is approaching π.

In Figures 5.1 and 1 we present the density and the distribution functions, respectively, of I_1 computed with the Euler algorithm. It has been checked that the PDE method yields the same results. However, the convergence in the case $\mu = 0.3$ seems to be slow. In fact, for $\mu = 0.1$ the convergence rate of the PDE method is so slow that we were unable to get satisfactory results with our limited computation capacity (RAM).

Example 5.2. In this example we compare the functionals

$$I_2 := \int_0^\infty \exp(-2B_s^{(\mu,\sigma)})ds \quad \text{and} \quad I_3 := \int_0^\infty (\exp(B_s^{(\mu,\sigma)}) + 1)^{-2} ds.$$

Notice that

$$I_3 = \int_0^\infty \exp(-2B_s^{(\mu,\sigma)})\, \frac{1}{(1+\exp(-B_s^{(\mu,\sigma)}))^2}\, ds,$$

hence I_3 may be seen as a modification of I_2 which does not allow arbitrary large positive discounting. We remark also that I_3 has all moments which is not the case with I_2.

The Dufresne-Yor identity (cf. (1.2)) states that

$$I_2 = H_0(R^{(2-2\mu/\sigma^2)}) \qquad \text{a.s.},$$

where $R_0^{(2-2\mu/\sigma^2)} = 1/\sigma$. Consequently,

$$\mathbf{E}_0\left(\exp\left(-\rho\, I_2\right)\right) = \frac{\varphi_\rho(1/\sigma)}{\varphi_\rho(0)},$$

with (see [3] p. 133)

$$\varphi_\rho(x) = x^{-\nu}\, K_\nu(x\sqrt{2\rho}), \quad \text{and} \quad \varphi_\rho(0) = 2^{-(\nu+2)/2}\Gamma(-\nu)\, \rho^{\nu/2}$$

and $\nu = -\mu/\sigma^2$.

For I_3 we have the identity

$$I_3 = H_0(Z) \qquad \text{a.s.},$$

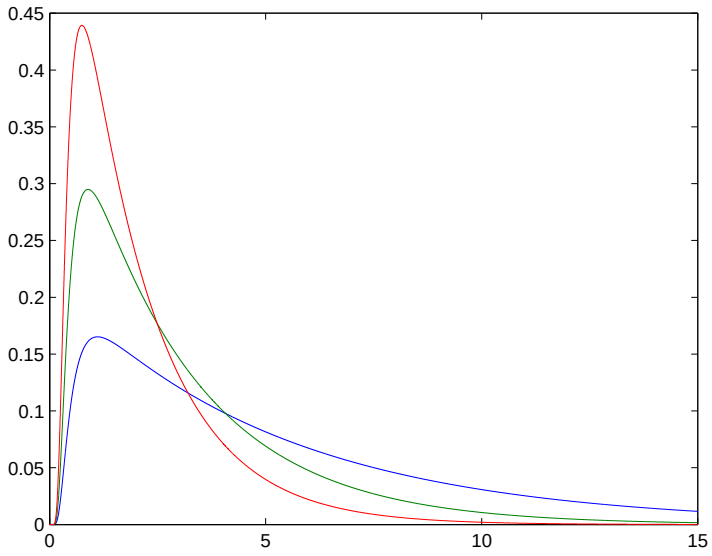

Figure 1: Density of $\int_0^\infty \cosh^{-2}(B_t^{(\mu)})\,dt$ for $\mu = 0.3$ (lowest peak), $\mu = 0.5$ and $\mu = 0.7$ (highest peak).

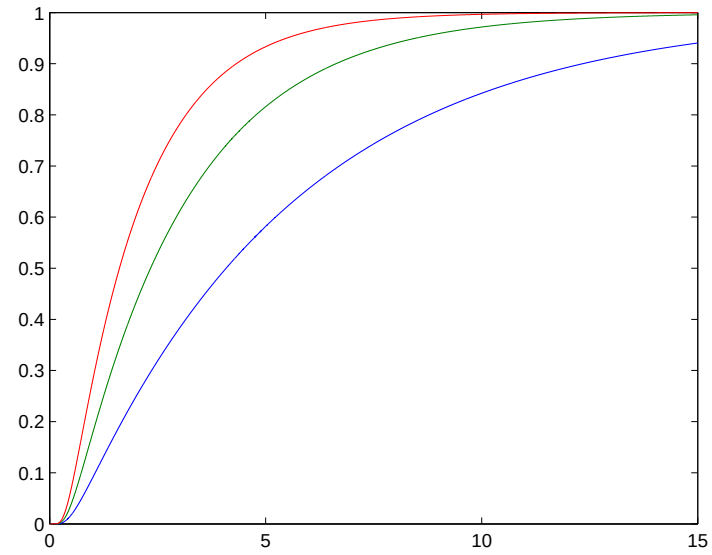

Figure 2: Distribution function of $\int_0^\infty \cosh^{-2}(B_t^{(\mu)})\,dt$ for $\mu = 0.3$ (lowest curve), $\mu = 0.5$ and $\mu = 0.7$ (highest curve).

where Z is the diffusion associated with the SDE

$$dZ_t = dB_t + \left(\mu + (\mu - \frac{1}{2})\frac{\exp(Z_t)}{1-\exp(Z_t)}\right)\, dt, \qquad Z_0 = -\log 2.$$

Notice that here $g(x) := -\log(1+\exp(-x))$ (cf. Proposition 2.1) and that Z lives on $\mathbf{R}_-$. From [4] we recall the Laplace transform

$$\mathbf{E}_0\Big(\exp\Big(-\rho\, I_3\Big)\Big) = K\ 2^{\,\mu-\sqrt{\mu^2+2\rho}}\ {}_2F_1(\alpha,\beta,\alpha+\beta+2\mu\,;1/2),$$

where

$$\alpha = \frac{1}{2} - \mu + \sqrt{\mu^2+2\rho} + \sqrt{\frac{1}{4}+2\rho}, \quad \beta = \frac{1}{2} - \mu + \sqrt{\mu^2+2\rho} - \sqrt{\frac{1}{4}+2\rho},$$

and

$$K = \frac{\Gamma\,(2\mu+\alpha)\ \Gamma\,(2\mu+\beta)}{\Gamma(2\mu+\alpha+\beta)\ \Gamma(2\mu)}.$$

See Figures 3, 4, 5 and 6 for illustrations of the distributions of I_2 and I_3 computed with the Euler algorithm.

For both functionals in this example it was possible to solve the corresponding PDE numerically for $\mu \geq \frac{1}{2}$. For $\mu < 1/2$ the drift term tends to $-\infty$ as Z approaches the killing boundary 0. This again leads to very slow convergence. While it was still possible to achieve good results for some choices of $\mu < \frac{1}{2}$, for a small enough μ the results were bad even with the finest grid we could run on the computer. Notice that here we also need to truncate the semi-infinite domains into finite ones for numerical computations. This did not constitute a major problem, but with larger domains it is difficult to achieve (depending on the computer capacity) a grid which is spatially dense enough for accurate computations.

Example 5.3. We define the one-sided variants of I_2 and I_3 via

$$I_4 := \int_0^\infty \exp(-2B_s^{(\mu,\sigma)})\mathbf{1}_{\{B_s^{(\mu,\sigma)}>0\}}ds$$

and

$$I_5 := \int_0^\infty (\exp(B_s^{(\mu,\sigma)})+1)^{-2}\mathbf{1}_{\{B_s^{(\mu,\sigma)}>0\}}ds,$$

respectively.

In [24] it is shown that

$$I_4 = H_{1/\sigma}(R^{(2\mu/\sigma^2)}) \qquad \text{a.s.}$$

where $R_0^{(2\mu/\sigma^2)} = 0$. The Laplace transform of I_4 is hence given by

$$\mathbf{E}_0\left(\exp\Big(-\rho\, I_4\Big)\right) = \frac{\psi_\rho(0)}{\psi_\rho(1/\sigma)},$$

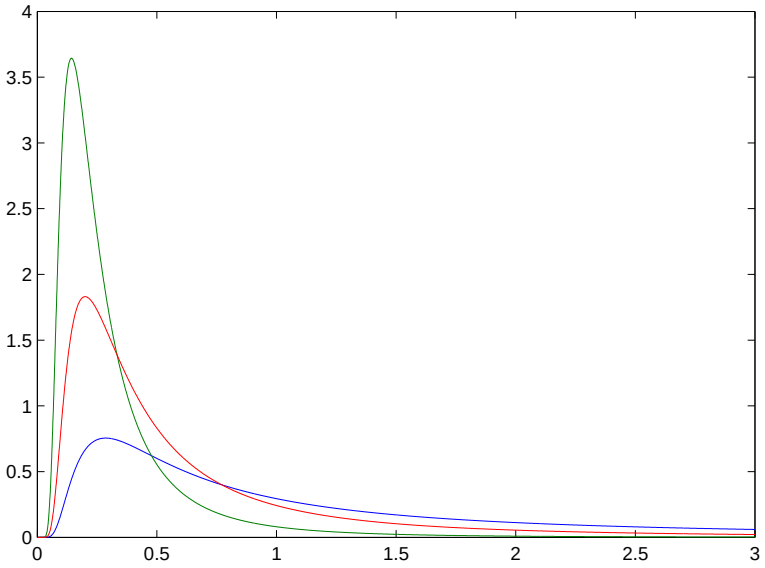

Figure 3: Density of $\int_0^\infty \exp(-2\,B_t^{(\mu)})\,dt$ for $\mu = 0.75$ (lowest peak), $\mu = 1.50$ and $\mu = 2.50$ (highest peak).

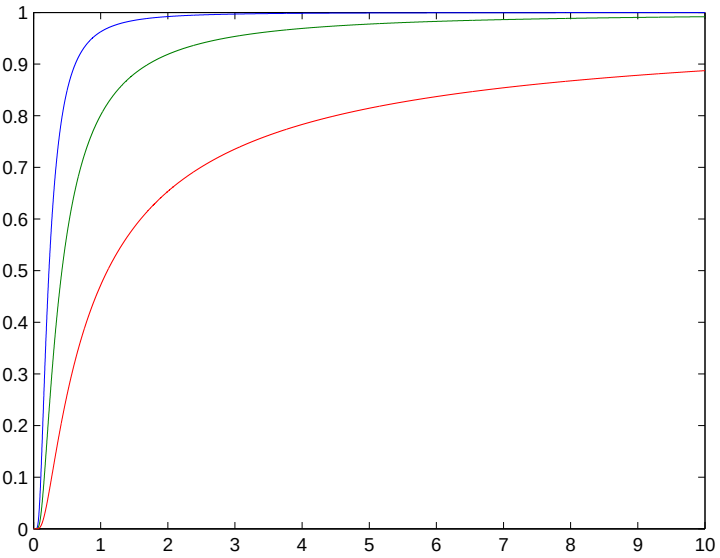

Figure 4: Distribution function of $\int_0^\infty \exp(-2\,B_t^{(\mu)})\,dt$ for $\mu = 0.75$ (lowest curve), $\mu = 1.50$ and $\mu = 2.50$ (highest curve).

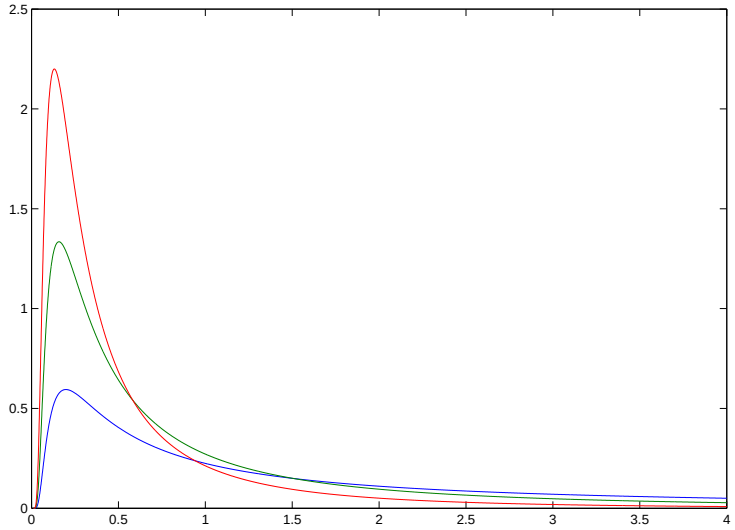

Figure 5: Density function of $\int_0^\infty (\exp(\, B_t^{(\mu)}) + 1)^{-2}\, dt$ for $\mu = 0.25$ (lowest peak), $\mu = 0.50$ and $\mu = 0.75$ (highest peak).

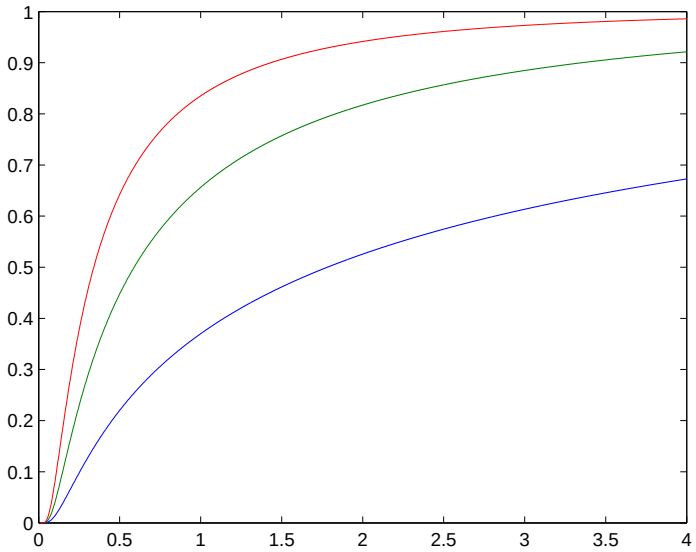

Figure 6: Distribution function of $\int_0^\infty (\exp(\, B_t^{(\mu)}) + 1)^{-2}\, dt$ for $\mu = 0.25$ (lowest curve), $\mu = 0.50$ and $\mu = 0.75$ (highest curve).

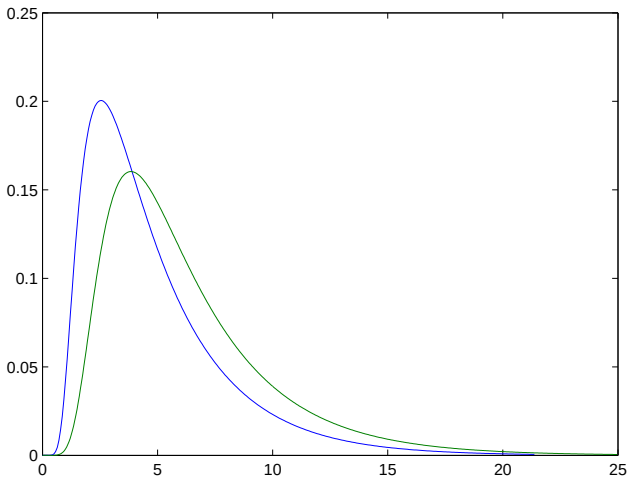

Figure 7: Density function of $\int_0^\infty (\exp(\,B_t^{(\mu,\sigma)}) + 1)^{-2}\,\mathbf{1}_{\{B_t^{(\mu,\sigma)}>0\}}\,dt$ (upper peak) compared with the density function of $\int_0^\infty \exp(-2\,B_t^{(\mu,\sigma)})\,\mathbf{1}_{\{B_t^{(\mu,\sigma)}>0\}}\,dt$ for $\mu = 0.04$ and $\sigma = 0.20$.

with (see [3] p. 133)

$$\psi_\rho(x) = x^{-\nu}\,I_\nu(x\sqrt{2\rho}) \quad \text{and} \quad \psi_\rho(0) = \frac{\rho^{\nu/2}}{2^{\nu/2}\,\Gamma(\nu+1)}$$

and $\nu = \mu/\sigma^2 - 1$.

The Laplace transform of the functional I_5 (in [24] this is called the one-sided translated Dufresne functional) is not known but the following identity (see [24]) holds

$$I_5 = H_0(Z) \qquad \text{a.s.},$$

where Z is a diffusion associated with the generator

$$\mathcal{G}f(x) = \frac{1}{2}\frac{d^2 f}{dx^2}(x) + \left(\frac{1}{2}\sigma + \frac{\mu - \frac{1}{2}\sigma^2}{\sigma\,(1-\exp(\sigma x))}\right)\frac{d\,f}{dx}(x)$$

living on $[-(\log 2)/\sigma, 0)$, having $-(\log 2)/\sigma$ as a reflecting barrier, and 0 as a killing barrier.

In Figure 7 we compare the densities of I_4 and I_5 (see [9] for comparisions between I_2 and I_4). The density and distribution functions of I_5 are displayed for different values of μ and σ in Figures 8 and 9.

Example 5.4. In our final example we consider the functional

$$I_6^{(\delta)} := \int_0^\infty \exp(-2\,R_s^{(\delta)})ds, \quad \delta \geq 2.$$

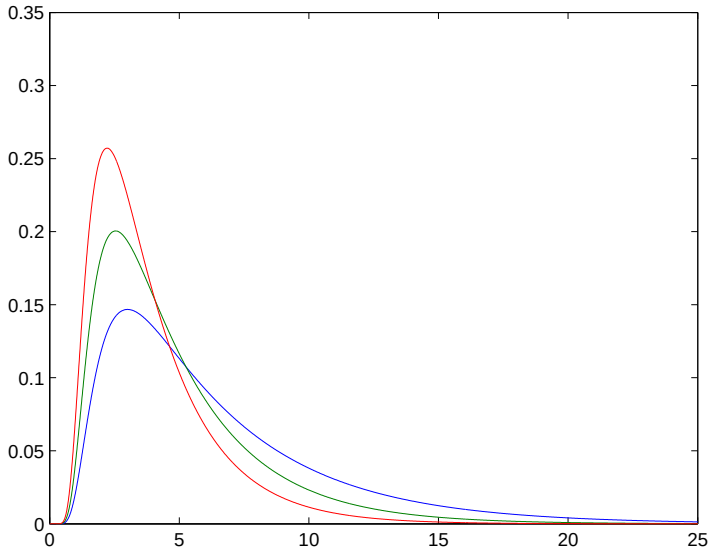

Figure 8: Density function of $\int_0^\infty (\exp(\, B_t^{(\mu,\sigma)}) + 1)^{-2}\, \mathbf{1}_{\{B_t^{(\mu,\sigma)} > 0\}}\, dt$ for $\sigma = 0.20$ and $\mu = 0.03$ (lowest peak), $\mu = 0.04$, and $\mu = 0.05$ (highest peak)

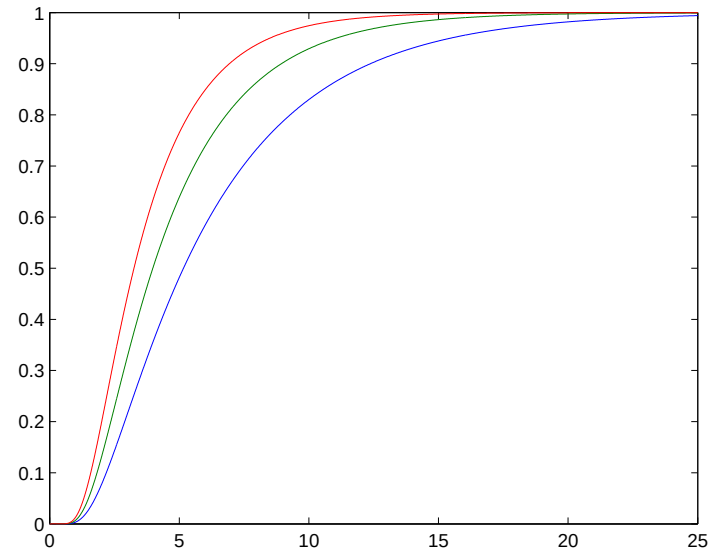

Figure 9: Distribution function of $\int_0^\infty (\exp(\, B_t^{(\mu,\sigma)}) + 1)^{-2}\, \mathbf{1}_{\{B_t^{(\mu,\sigma)} > 0\}}\, dt$ for $\sigma = 0.20$ and $\mu = 0.03$ (lowest curve), $\mu = 0.04$, and $\mu = 0.05$ (highest curve)

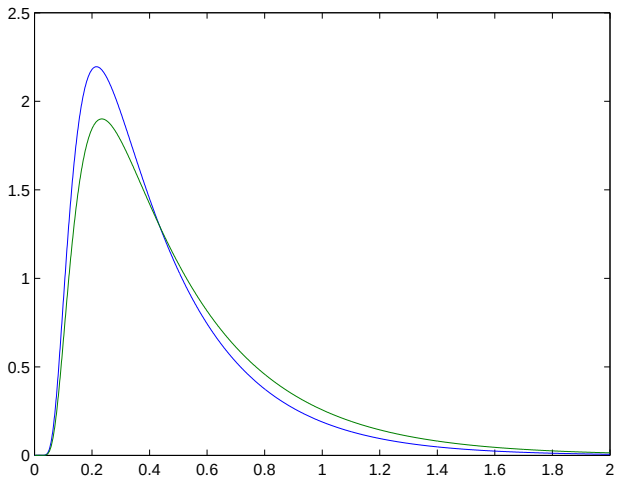

Figure 10: Density function of $\int_0^\infty \exp(-2\,R_t^{(\delta)})\,dt$ for $\delta = 3.0$ (upper peak) obtained using the drift $\frac{1}{2x}(1+\frac{\delta-1}{\log x})$ compared with the correct one (lower peak).

Proposition 2.1 when applied for $R^{(\delta)}$ and $g(x) := \exp(x)$ leads us to the identity

$$I_6 = H_0(Z) \qquad \text{a.s.} \tag{5.2}$$

with Z a diffusion associated with the SDE

$$dZ_t = dB_t + \frac{1}{2\,Z_t}\left(1+\frac{\delta-1}{\log Z_t}\right)dt, \qquad Z_0 = 1. \tag{5.3}$$

In the case $\delta = 3$ it is known (see Legall [17] and also [24]) that

$$I_6^{(3)} = H_1(R^{(2)}) \qquad \text{a.s.} \tag{5.4}$$

with $R_0^{(2)} = 0$.

Since we do not have an expression for the Laplace transform of $I_6^{(\delta)}$ for $\delta \neq 3$ we solve numerically the associated PDE. Unfortunately, due to the complexity of the drift term (in particular, notice that this tends, for all values on $\delta \geq 2$, to $+\infty$ in the vicinity of $0+$) simple finite difference schemes do not seem to give solutions converging to the correct one, see Figure 10. In search for improvement we implemented a nonuniform grid making the spatial discretization denser near the boundaries, and used a fourth-order implementation at the Neumann boundary. While this yielded better results than what is seen in Figure 10, full convergence still remained out of reach.

These difficulties can at least partly be overcome by transforming the diffusion Z given via SDE (5.3). Indeed, we study now the h-transform of Z with $h(x) = S(x) - S(0)$ where S is the scale function of Z Straightforward computations (cf. [3] p. 17) show that we may take

$$S(x) = \frac{1}{\delta-2}\,|\log x|^{2-\delta}, \quad 0 < x < 1$$

(for simplicity we consider only the case $\delta > 2$). Then

$$\lim_{x\to 0} S(x) = 0 \quad \text{and} \quad S'(x) = x^{-1}|\log x|^{1-\delta}.$$

Consequently, the generator of the h-transform is given by

$$\begin{aligned}\mathcal{G}^{\uparrow} f &= \frac{1}{2}\frac{d^2 f}{dx^2} + \frac{1}{2x}\left(1 + \frac{\delta - 1}{\log x}\right)\frac{df}{dx} + \frac{S'(x)}{S(x)}\frac{df}{dx} \\ &= \frac{1}{2}\frac{d^2 f}{dx^2} + \frac{1}{2x}\left(1 + \frac{3 - \delta}{\log x}\right)\frac{df}{dx}, \qquad 0 < x < 1.\end{aligned}$$

Let $Z^{\uparrow}$ denote the h-transform, i.e., $Z^{\uparrow}$ is the diffusion associated with the generator $\mathcal{G}^{\uparrow}$. By Williams [30] time reversal result (see [3] p. 35, also for further references)

$$H_0(Z) \overset{(\mathrm{d})}{=} H_1(Z^{\uparrow}).$$

The PDE associated with $Z^{\uparrow}$ seems to be well suited for numerical computations. Notice, in particular, that if $\delta > 3$ the drift term of $Z^{\uparrow}$ tends to $+\infty$ as $x \to 1$ which fact is in strong contrast with the corresponding behaviour of the drift term of Z. Hereby it is also of interest to classify the boundaries of Z and $Z^{\uparrow}$. It holds for Z that the boundary point 0 is exit-not-entrance and 1 is entrance-not-exit. For the process $Z^{\uparrow}$ we have that 0 is entrance-not-exit and 1 is entrance-exit (regular) if $2 < \delta < 4$ and entrance-not-exit if $\delta \geq 4$. Figures 11, 12 show the density and distribution functions of I_6 for some choises of δ computed from the PDE associated with $Z^{\uparrow}$.

As a final comment, and as an extra bonus from our transformation, we remark that when $\delta = 3$ then $\mathcal{G}^{\uparrow}$ is the generator of $R^{(2)}$, and we have recovered the identity (5.4).

Acknowledgements. Paavo Salminen thanks Vadim Linetsky for information on numerical inversion of Laplace transforms of hitting times. Olli Wallin thanks Siddhartha Mishra for several useful discussions on numerical solution of partial differential equations.

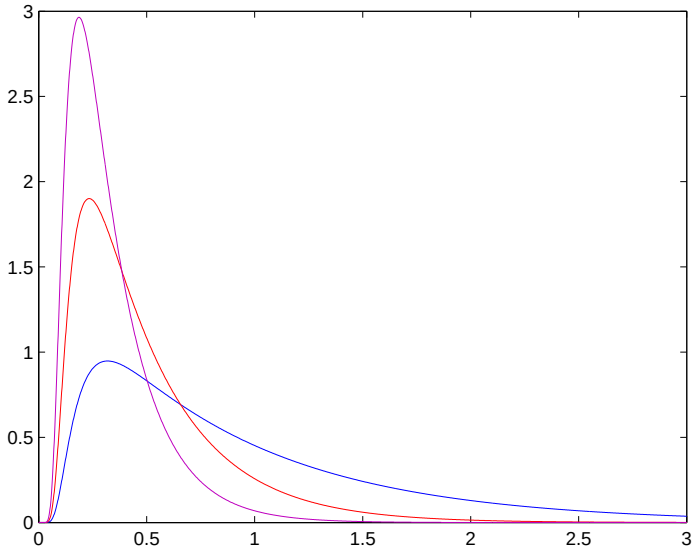

Figure 11: Density function of $\int_0^\infty \exp(-2\,R_t^{(\delta)})\,dt$ for $\delta = 2.5$ (lowest peak), $\delta = 3.0$, $\delta = 3.5$ (highest peak).

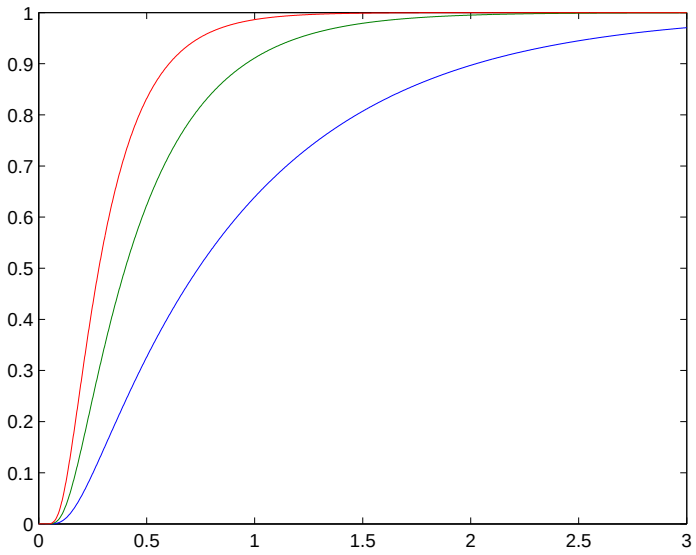

Figure 12: Distribution function of $\int_0^\infty \exp(-2\,R_t^{(\delta)})\,dt$ for $\delta = 2.5$ (lowest curve), $\delta = 3.0$, $\delta = 3.5$ (highest curve).

References

[1] J. Abate and W. Whitt. Numerical inversion of Laplace transforms of probability distributions. *ORSA Journal of Computing*, 7(1):36–43, 1995.

[2] R.M. Blumenthal and R.K. Getoor. *Markov Processes and Potential Theory*. Academic Press, New York, London, 1968.

[3] A.N. Borodin and P. Salminen. *Handbook of Brownian Motion – Facts and Formulae, 2nd edition*. Birkhäuser, Basel, Boston, Berlin, 2002.

[4] A.N. Borodin and P. Salminen. On some exponential integral functionals of BM(μ) and BES(3). *Zap. Nauchn. Semin. POMI*, 311:51–78, 2004. Preprint available in http://arxiv.org/abs/math.PR/0408367.

[5] D. Britz, O. Østerby, and J. Strutwolf. Damping of Crank-Nicolson error oscillations. *Computational Biology and Chemistry*, 27:253–263, 2003.

[6] P. Carr and V. Linetsky. The valuation of executive stock options in an intensity-based framework. *European Finance Review*, 4:211–230, 2000.

[7] D. Davydov and V. Linetsky. Pricing and hedging path dependent options under the CEV process. *Management Science*, 47(7):949–965, 2001.

[8] D. Davydov and V. Linetsky. Structuring, pricing and hedging double barrier step options. *J. Comput. Finance*, 5(2):55–87, 2001/02.

[9] M. Decamps, A. De Schepper, M. Goovaerts, and W. Schoutens. A note on some new perpetuities. *Scand. Actuarial J.*, pages 261–270, 2005(4).

[10] D. Dufresne. The distribution of a perpetuity, with applications to risk theory and pension funding. *Scand. Actuarial J.*, 1-2:39–79, 1990.

[11] H.J. Engelbert and T. Senf. On functionals of Wiener process with drift and exponential local martingales. In M. Dozzi, H.J. Engelbert, and D. Nualart, editors, *Stochastic processes and related topics. Proc. Wintersch. Stochastic Processes, Optim. Control, Georgenthal/Ger. 1990*, number 61 in Math. Res., Academic Verlag, pages 45–58, Berlin, 1991.

[12] W. Feller. The parabolic differential equations and the associated semi-groups of transformations. *Ann. Math.*, 55(3):468–519, 1952.

[13] M. Fu, D. Madan, and T. Wang. Pricing asian options: a comparison of analytical and monte carlo methods. *J. Comput. Finance*, 2:49–74, 1997.

[14] Gary W. Harrison. Numerical solution of the Fokker Planck equation using moving finite elements. *Numerical methods for Partial differential Equations*, 4:219–232, 1988.

[15] K. Itô and H.P. McKean. *Diffusion Processes and Their Sample Paths*. Springer Verlag, Berlin, Heidelberg, 1974.

[16] J. Kent. Eigenvalue expansions for diffusion hitting times. *Z. Wahrscheinlichkeitstheorie verw. Gebiete*, 52:309–320, 1980.

[17] J.F. LeGall. Sur la mesure de Hausdorff de la courbe brownienne. In J. Azéma and M. Yor, editors, *Séminaire de Probabilités XIX*, number 1123 in Springer Lecture Notes in Mathematics, pages 297–313, Berlin, Heidelberg, New York, 1985.

[18] H.P. McKean. Elementary solutions for certain parabolic differential equations. *TAMS*, 82:519–548, 1956.

[19] H.P. McKean. *Stochastic Integrals*. Academic Press, New York, London, 1969.

[20] M.A. Milevsky. The present value of stochastic perpetuity and the Gamma distribution. *Insur. Math. Econ.*, 20:243–250, 1997.

[21] R.Poulsen. Approximate maximum likelihood estimation of discretely observed diffusion processes. *CAF working paper series*, 29, 1999.

[22] P. Salminen and M. Yor. A note on a.s. finiteness of perpetual integral functionals of diffusions. *PMA preprint series, Paris VI (submitted for publication)*.

[23] P. Salminen and M. Yor. On Dufresne's perpetuity, translated and reflected. In J. Akahori, S. Ogawa, and S. Watanabe, editors, *Proceedings of Ritsumeikan International Symposium: Stochastic Processes and Applications to Mathematical Finance*, Singapore, 2004. World Scientific Publishing Co.

[24] P. Salminen and M. Yor. Perpetual integral functionals as hitting times and occupation times. *Elect. J. Prob.*, 10:371–419, 2005.

[25] P. Salminen and M. Yor. Properties of perpetual integral functionals of Brownian motion with drift. *Ann. I.H.P.*, 41(3):335–347, 2005.

[26] A. De Schepper, M. Goovaerts, and F. Delbaen. The Laplace transform of annuities certain with exponential random time. *Insur. Math. Econ.*, 11(4):291–294, 1992.

[27] J. Strikwerda. *Finite difference schemes and aprtial differential equations*. Wadsworth & Brooks/Cole, Pacific Grove, CA, 1989.

[28] J.W. Thomas. *Numerical partial differential equations: finite difference methods*. Springer Verlag, New York, 1995.

[29] I.V. Vagurina. On diffusion processes corresponding to hypergeometric equation. *Zap. Nauchn. Semin. POMI*, 311:79–91, 2004.

[30] D. Williams. Path decompositions and continuity of local time for one-dimensional diffusions. *Proc. London Math. Soc.*, 28:738–768, 1974.

[31] M. Yor. Sur certaines fonctionnelles exponentielles du mouvement brownien réel. *J. Appl. Probab.*, 29:202–208, 1992, (translated in English in [32].

[32] M. Yor. *Exponential functionals of Brownian motion and related processes* in series Springer Finance. Springer Verlag, Berlin, Heidelberg, New York, 2001.